2012

Numerical Study of Convective Heat Transfer for Flat Unglazed Transpired Solar Collectors

Siwei Li
li613@purdue.edu

Panagiota Karava

Numerical Study of Convective Heat Transfer for Flat Unglazed Transpired Solar Collectors

Siwei LI[1], Panagiota KARAVA[2*]

[1]Purdue University, School of Civil Engineering,
West Lafayette, Indiana, USA
Contact information (+1-765-494-1714, li613@purdue.edu)

[2]Purdue University, School of Civil Engineering and Division of Construction Engineering and Management,
West Lafayette, Indiana, USA
Contact information (+1-765-494-4573, +1-765-494-0644, pkarava@purdue.edu)

* Corresponding Author

ABSTRACT

Convective heat transfer coefficients (CHTC) for flat unglazed transpired solar collectors have been computed using high-resolution 3-dimensional steady RANS CFD simulations. The Standard k-ε, Renormalization Normal Group k-ε (RNG k-ε), Realizable k-ε and Shear Stress Transport k-ω (SST k-ω) turbulence closure models were used and the results were compared with experimental data from the literature. The validation study showed that both the Standard k-ε and the RNG k-ε model performed better in terms of matching the experimental data and showing consistently faster convergence. Local CHTC along the plate were evaluated with the validated model for different suction flow rates (0.0448 to 0.0688 m/s) and free stream turbulence intensity (0.8% and 20%) at 6 m/s approaching flow velocity with the results showing that the turbulence intensity has a more profound impact on the overall convective heat transfer process. The local CHTC in the solid surface region of the collector remains constant after a certain length for the cases considered; however, the starting length was found to be longer compared to the values reported in previous analytical studies.

1. INTRODUCTION

Unglazed transpired solar collectors (UTCs) consist of dark porous cladding installed as the exterior layer of the building envelope (normally roof or facade) with a narrow gap beneath it. The cladding absorbs solar radiation, thus heating up the air flowing through the perforations driven by a suction fan. UTC's can be integrated with Photovoltaic systems, thereby generating electricity and heat, resulting in overall efficiencies that can be up to 70% (Athienitis et al. 2010; Bambara et al. 2012). In these systems, the hot air is collected at the outlet and it can be used to preheat ventilation air, fed into an air source heat pump to preheat domestic hot water and/or provide cooling using desiccants or absorption technology, thus satisfying part of the building's heating and cooling requirements.

An important parameter that determines the performance and efficiency of UTC's is the convective heat transfer coefficient (CHTC) between the heated plate and the ambient air due to the wind flow over the collector. Previous studies on CHTC for UTC's (Kutscher 1992; Golneshan 1993; Van Decker et al. 2001; Gawlik 1993) mainly focused on analytical and experimental investigations due to the lack of advanced computational techniques. Schlichting and Gersten (2000) pointed out that continuous suction provides stability to the flow over a flat plate, raising the critical Reynolds number by a factor of 130. For laminar, uniform approaching flow, the boundary layer thickness is constant after the starting length; thus the Reynolds number based on boundary layer thickness and wind speed will no longer increase. If this Reynolds number is below 70,000, transition to turbulence on a smooth plate with uniform suction will not occur, regardless of the plate length.

Kutscher (1992) and Kutscher et al. (1993) demonstrated an analytical solution of the Navier-Stokes equations for flow over a flat perforated plate with homogeneous suction, which means that the perforation spacing distance is smaller than the boundary layer thickness (normally with a magnitude of a few mm). Results showed that the velocity and thermal boundary layer thickness remain constant along the plate after the starting length and the convective heat loss from the plate due to the wind flow is quite small as the heat will be recaptured when the ambient air is drawn into the gap. This solution implies that the CHTC along the plate remains constant for given conditions. However, it is only valid for laminar, uniform approaching flow conditions and homogeneous suction, which may be an oversimplification, for the analysis of transpired solar collectors mounted on surfaces of buildings, which are immersed in the atmospheric boundary layer. Moreover, the low porosity and large perforation spacing distance of UTCs would typically result in discrete suction rather than homogeneous suction.

Kutscher (1992; 1994) conducted experiments to evaluate the overall convective heat transfer process for UTCs subjected to uniform approaching flow with turbulence intensity of 0.8% and the following empirical correlation was obtained for the average Nu_D of the entire plate:

$$Nu_D = 2.75[\left(\frac{P}{D}\right)^{-1.2} Re_D^{0.43} + 0.011\sigma Re_D \left(\frac{U_\infty}{V}\right)^{0.48}] \quad (1)$$

where Nu_D is based on the perforation diameter; P is the pitch length; D is the perforation diameter; Re_D is based on the suction velocity and perforation diameter; σ is the plate porosity; U_∞ is the wind speed; and V is the suction velocity. A few numerical studies followed the work by Kutscher (1992) limited the studied geometry to a pitch by assuming that UTCs are a combination of multiple pitches with similar thermal performance. For example, Arulanandam et al. (1999) simulated a quarter of pitch under no wind condition using a laminar Computational Fluid Dynamics (CFD) model and obtained a Nu number correlation including the suction flow rate, perforation diameter, as well as the plate thickness, admittance and porosity. However, to the authors' best knowledge, there is no previous study in the literature that has investigated the convective heat transfer process for the entire perforated plate subjected to turbulent approaching flow conditions.

The rapid development of computational power and speed makes CFD techniques a powerful alternative for further investigation of convective heat transfer on UTCs, eliminating difficulties associated with the impact of radiation and the precise control of experimental conditions, which requires considerable time and cost for an accurate data acquisition process. By solving the conservation equations of mass, momentum and energy, CFD can provide quantitative answers for various airflow and heat transfer parameters in this system when properly validated. It offers a higher degree of flexibility and detail, i.e. it can distinguish convective heat transfer from radiation and it can provide local convective heat transfer coefficients.

The overall goal of this research program is to develop models for the design and analysis of building-integrated photovoltaic/thermal systems combined with transpired air collectors. The present study is the first step in this direction and the objective is (a) to test the accuracy of different CFD models in evaluating the complex convective heat transfer process on UTCs; and (b) to compute average and local CHTC for horizontally placed UTCs under turbulent approaching flow conditions. The main parameters considered in this study are the wind speed (approaching flow velocity), suction flow rate and turbulence intensity.

2. NUMERICAL APPROACH

The commercial CFD software, ANSYS (version 13.0) was used to conduct all the simulations and Gambit 2.4.6 was used to develop the geometry model, which is shown in Figure 1. In the region above the plate, the left side of the domain was defined as the velocity-inlet with a specified approaching flow velocity and the right side of the domain was defined as the pressure-outlet with zero gauge pressure. The plate was set to be a wall with thickness of 0.00086m and the perforations on the plate were set to be 'interior'. The bottom of the cavity was defined as velocity-outlet with a specified suction velocity. The left and right side of the cavity were defined as adiabatic walls. A symmetry boundary condition was used for all other faces, which means zero velocity and temperature gradient. The upper domain is 0.3m height, which is sufficient for the boundary layer growth.

The plate is divided into two parts in the stream-wise direction: a perforation row and a solid row. The perforation row includes all the perforations and can be considered as a 'discrete suction' component. The solid row covers

more than 90% of the plate area and it is similar to a smooth, impermeable flat plate, but the flow is different from the classical flat plate case due to the suction created by the perforation row. A perforated plate with an area of 0.6m x 0.6m and a cavity with 0.15m height were considered. The plate has pitch length of 0.01689 m and perforation diameter of 0.00159 m. Considering the small size of the perforations , their shape was assumed to be square, instead of the circular shape used in the experiments (Van Decker et al., 2001), for model simplicity. The simulated solar radiation in the experiments was around 600W/m^2, the ambient air temperature 298K, and the turbulence intensity of incoming flow 0.8%, which is considered to be uniform. These values were used as inputs in the CFD model.

The Standard k-ε, Renormalization Normal Group k-ε (RNG k-ε), Realizable k-ε and Shear Stress Transport k-ω (SST k-ω) turbulence closure models available in ANSYS with Low Reynolds Number Correction were applied to a 3-dimensional computational domain. A second order upwind scheme was adopted for all the variables except pressure. The discretization of pressure is based on a staggered scheme. The SIMPLE algorithm was used to couple the pressure and momentum equations. If the sum of absolute normalized residuals for all the cells in flow domain became less than 10^{-6} for energy, 10^{-4} for other variables, the solution was considered converged. In all simulations, the y+ value is maintained around 1to satisfy the enhanced wall treatment requirement.

The grid independence for each case was verified using three different grids to ensure that grid resolution would not have a notable impact on the results. The results of the grid independence study are listed in Table 1. The difference between each grid is less than 1%, thus Grid 2 was selected for the simulations.

Table 1 Grid independence study

Plate temperature / Cavity outlet temperature [K]	Cell numbers			**Experimental data**
	Grid 1 (338232)	Grid 2 (416352)	Grid 3 (789270)	
Case 1: wind speed=1m/s, suction velocity=0.0688m/s	315.0/306.1	313.5/306.1	314.7/305.9	**313.9/306.5**
Case 2: Wind speed=0, Suction velocity=0.0564m/s	315.7/305.2	313.6/305.2	315.4/305.2	**312.9/305.3**

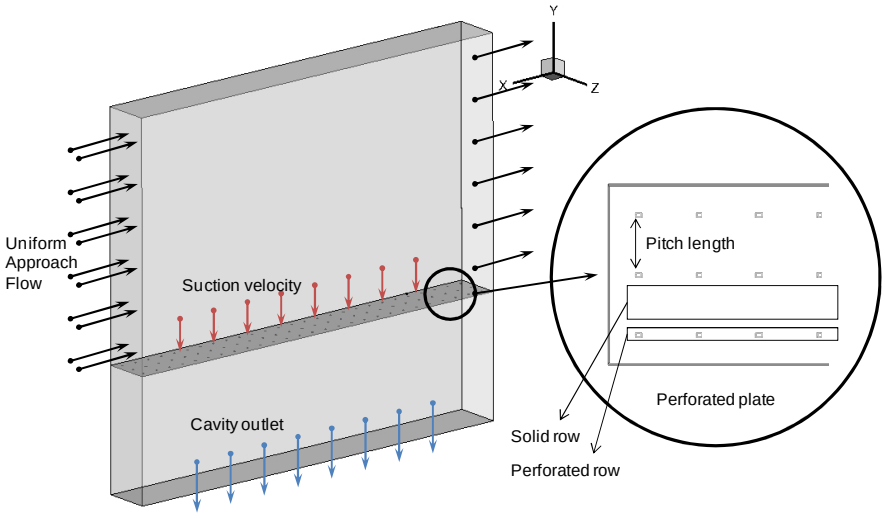

Figure 1 Computational domain

Table 2 Tested cases for model validation

Cases	**1**	**2**	**3**	**4**	**5**
Wind speed [m/s]	0	0	1	1	1
Suction velocity [m/s]	0.0564	0.0680	0.0448	0.0688	0.0774

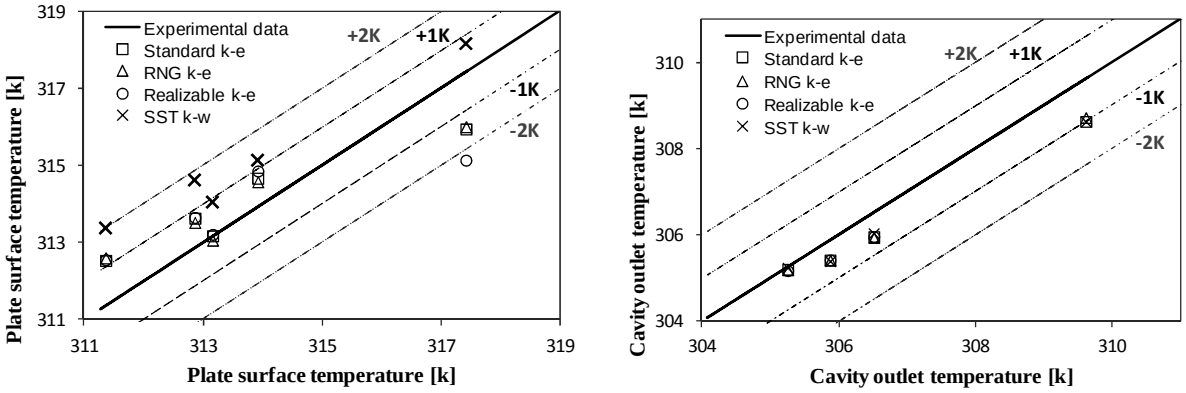

Figure 2 Comparison between CFD results and experimental data: (a) average plate surface temperature; (b) cavity outlet temperature

3. MODEL VALIDATION

The tested cases are listed in Table 2. The average plate surface temperature and cavity outlet temperature computed using different RANS models are compared with the experimental data and the results are shown in Figure 2 (a, b). For the plate surface temperature, the agreement between CFD results and experimental data is satisfactory with the error within 2 K. The Standard k-ε and the RNG k-ε model give similar results with the Realizable k-ε model but are more stable in terms of convergence and more consistent. The performance of the SST k-ω model is different than all the k-ε models with the results showing that surface temperature is overestimated.

For the cavity outlet temperature, all models provided identical results. Thus, based on this comparison, both the Standard k-ε and the RNG k-ε model can provide sufficiently accurate results for thermal modeling, however, the Standard k-ε model was adopted for the parametric study due to its slightly lower computing time and better convergence process.

The averaged Nusselt numbers for the entire plate (Nu_D) obtained from the CFD simulations are compared with the empirical correlation based on Eqn. (1) and results are shown in Figure 3 for four different suction velocities (0.0448m/s, 0.0564m/s, 0.0688m/s and 0.0774m/s) and three different wind speeds (1m/s, 4m/s and 6m/s). The numerical results compare relatively well with those obtained using the correlation with a maximum difference of 20%. These differences may be due to the staggered perforation arrangement used in the experiments (Kutscher, 1992).

4. RESULTS AND DISCUSSION

A parametric study was carried out for different approaching flow conditions with 0.8% and 20% turbulence intensity, a suction velocity of 0.0448m/s and 0.0688m/s and 6m/s wind speed. The perforation row and the solid row have been investigated separately as their flow features are dominated by different mechanisms. Results are plotted for the centerline of the perforation row, which crosses the center point of every perforation, as shown in Figure 4. However, the temperature and CHTC along the center line change periodically over each perforation due to suction, thus only the values for one point at 0.1mm after each perforation are plotted (point A). Similarly, results at the corresponding point B for the center line of the solid are shown in the following figures.

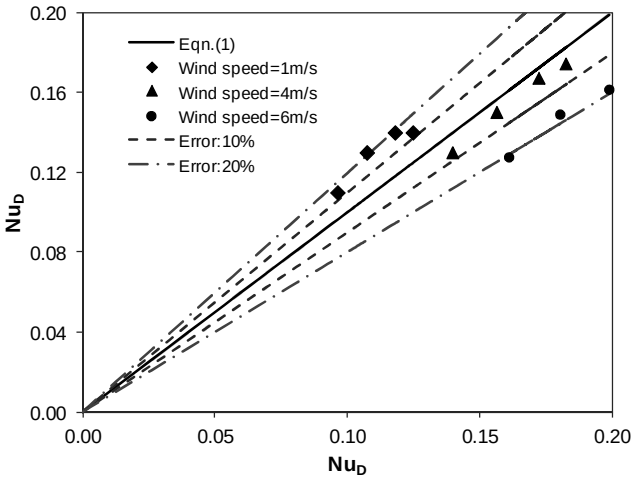

Figure 3 Comparison of average Nu_D obtained from the CFD simulations and the empirical correlation

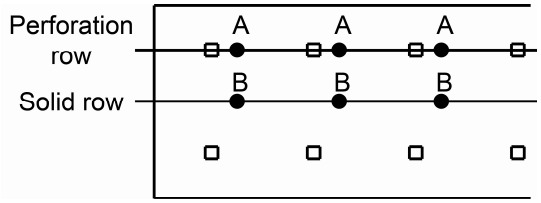

Figure 4 Configuration of the perforated plate with the points considered in the analysis

With regards to the solid row section, the upper two graphs in Figure 5 show that the vertical temperature profiles for same turbulence intensity are mostly identical regardless of the suction velocity; this indicates that turbulence intensity has a more pronounced impact on the temperature profile shape in the near wall region than the suction velocity which is expected as the suction areas are relatively small and aside of the solid row region. For the perforation row, the impact of suction velocity and turbulence intensity on the temperature profile is more complex. This is due to the fact that suction itself has the most significant impact on this region and the temperature profiles are more sensitive to the existence of suction rather than the actual velocity magnitude of the suction flow. To investigate the problem more closely, the thermal boundary layer thickness growth in the stream-wise direction is plotted in Figure 6. For the solid row region, the boundary layer thickness varies for approaching flow conditions with different turbulence intensity at the same suction velocity and wind speed. Also the thermal boundary layer is thicker for higher turbulence intensity as expected. However, for the perforation row, the boundary layer thickness is the same for both cases: TI=0.8% and TI=20%.

It should be also noted that for lower turbulence intensity (0.8%) the boundary layer thickness remains constant after x=0.35m, which indicates that the starting length is much longer than expected when analyzing this as a plate with homogeneous suction as suggested by Kutscher (1992). The contours presented in Figure 7 show the periodical behavior of CHTC over each perforation and also indicate that a constant CHTC is maintained after a certain starting length for TI=0.8%.

Based on the results displayed in Figure 8, it can be concluded that the impact of turbulence intensity dominates the overall heat transfer process as the solid row region covers more than 90% of the plate area. A constant CHTC is not observed in the perforation row, as expected, due to the decreased wind speed over this region caused by the suction. However, after x=0.3m the CHTC on the solid row region maintains a more constant value compared to the classic empirical correlation for a turbulent boundary layer flow over an impermeable flat plate (Incropera et al., 2006). For a constant heat flux boundary condition as implemented in UTC applications, constant CHTC implies constant surface temperature. Thus, for collectors with a large area, using an average CHTC or representing the surface

temperature with measured data from one location would provide sufficiently accurate results, as long as the measurement points are located after the starting length, which is found to be larger than the value reported in previous studies (i.e., 0.3 m in the present study as opposed to 0.06 m for collectors with homogeneous suction).

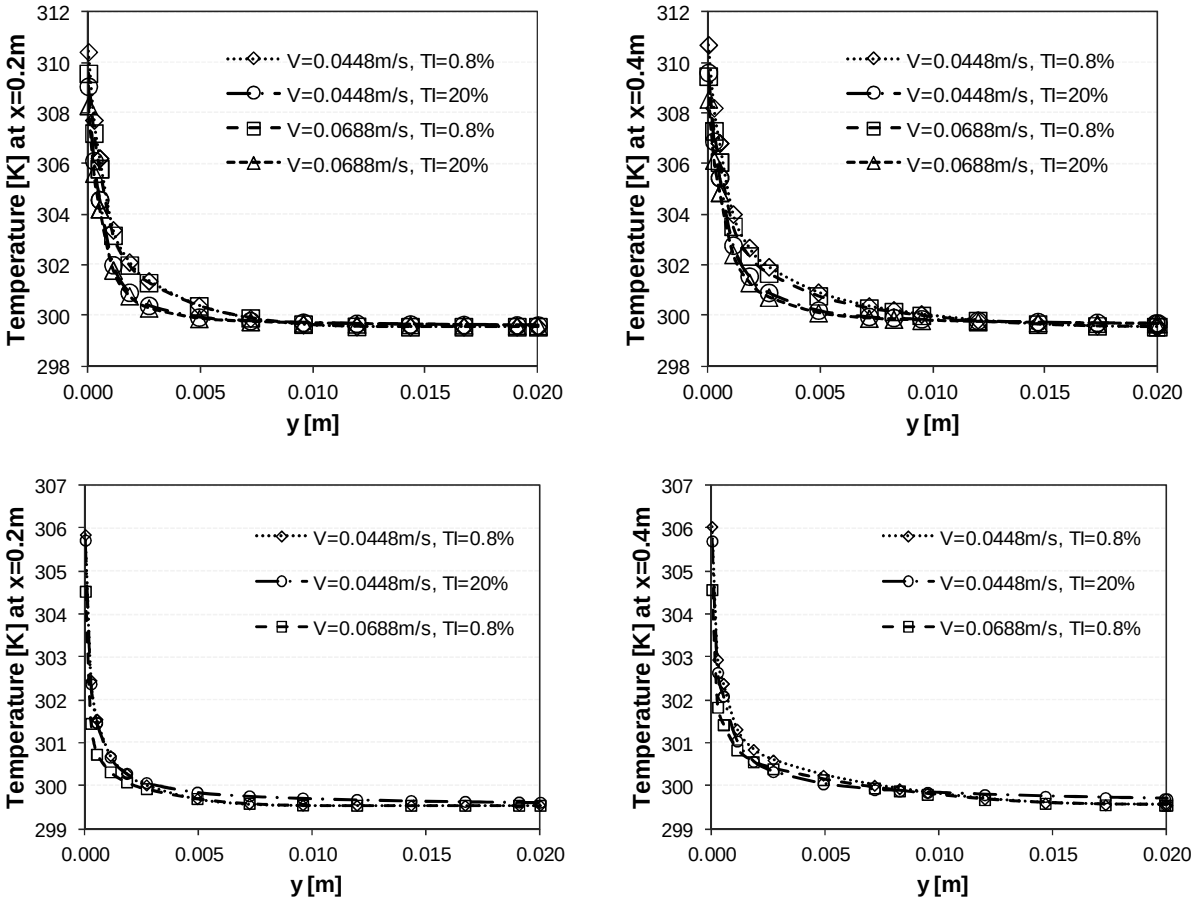

Figure 5 Boundary layer temperature profiles in the stream-wise direction for the solid row (top) and the perforation row (bottom)

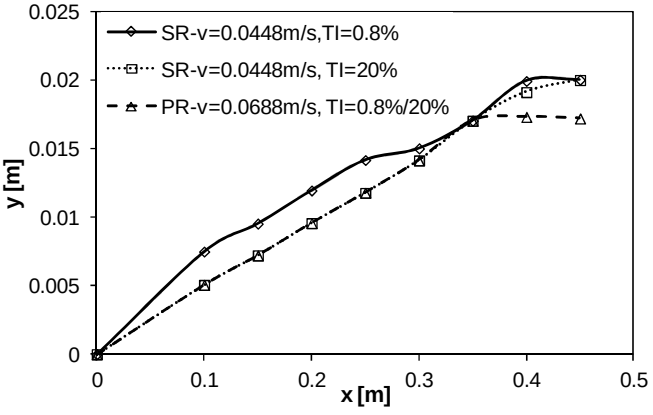

Figure 6 Thermal boundary layer growth along the stream-wise direction for different suction velocity and turbulence intensity at solid row (SR) and perforation row (PR)

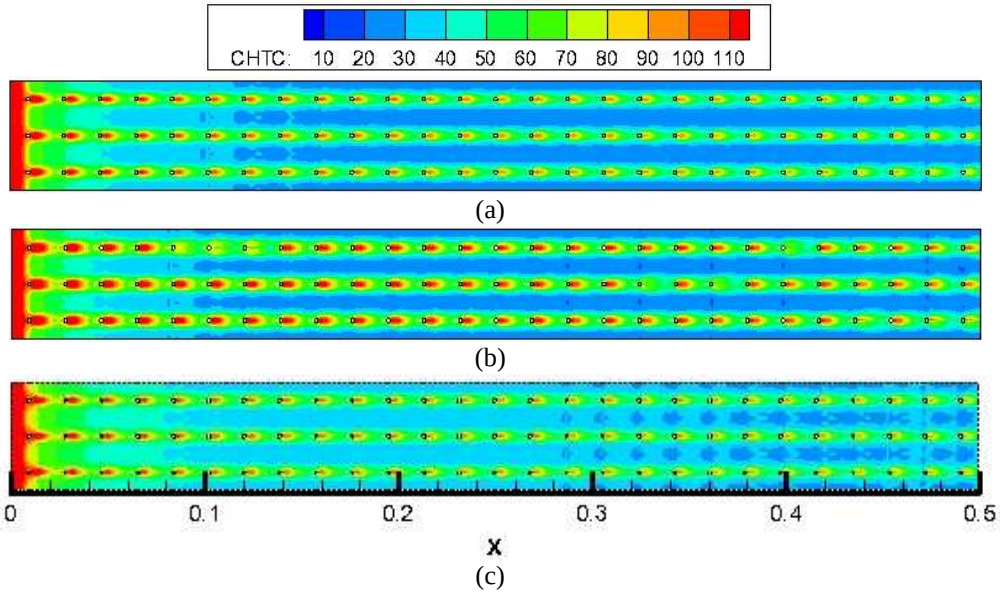

Figure 7 CHTC contour plot on the exterior surface of a perforated plate under wind speed of 6m/s for(a) Suction velocity = 0.0448 m/s, Turbulence intensity =0.8%; (b) Suction velocity=0.0688 m/s, Turbulence intensity =0.8%; and (c) Suction velocity=0.0448 m/s, Turbulence intensity =20%

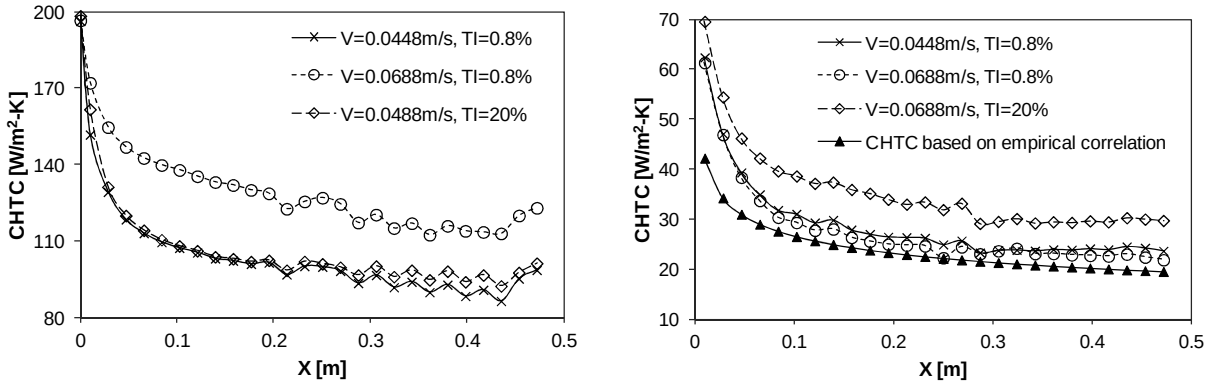

Figure 8 CHTC profile on the exterior surface of a perforated plate for 6m/s wind speed (a) perforation row (left); (b) solid row (right)

5. CONCLUSIONS

CFD simulations were performed to investigate the convective heat transfer process for an unglazed transpired solar collector. Numerical results for the surface and outlet air temperature were found to be in good agreement with previous experimental data, with an accuracy of 1K. Among all the turbulence models investigated, the Standard k-ε and the RNG k-ε model performed better with respect to accuracy and stability. By investigating the thermal boundary layer growth and the convective heat transfer along the plate for a perforation and a solid row separately, we found that although suction velocity effects the CHTC more in the perforation row, turbulence intensity has a more significant impact on the solid row and consequently on the average CHTC over the plate as the solid row covers a larger area. CHTC in the solid row region remains constant after a certain length; therefore the surface temperature and CHTC obtained after this length can be used to represent the surface temperature and CHTC of the entire plate with an acceptable accuracy. It should be noted that the starting length for discrete suction and turbulent approaching flow conditions is much longer than reported before. However, a more detailed analysis should be

conducted for a larger plate that is similar to those found in real applications. Also, other flow features such as impingement and separation as well as corrugated plate geometries integrated with Photovoltaic systems should be investigated to better understand the UTC performance.

REFERENCES

Arulanandam, S. J., Hollands, K. G. T. and Brundrett, E., 2000, A CFD heat transfer analysis of the transpired solar collector under no-wind condition, *Solar Energy*, vol. 67: p. 93–100.

Athienitis, A.K., Bambara, J., O'Neill, B. and Faille, J., 2011, A prototype photovoltaic/thermal system integrated with transpired collector, *Solar Energy*, vol. 85: p.139-153.

Bambara, J., Athienitis, A.K. and Karava, P., 2012, Performance Evaluation of a Building-Integrated Photovoltaic/Thermal System. Proceedings of International High Performance Buildings Conference at Purdue, July 16-19.

Gawlik, K.M., 1993, A numerical and experimental investigation of heat transfer issues in the practical utilization of unglazed, transpired solar air heaters. Ph.D. Thesis, Department of Civil, Environmental, and Architectural Engineering, University of Colorado, Colorado, USA.

Golneshan, A. A., 1994, Forced Convection Heat Transfer from Low Porosity Slotted Transpired Plates. Ph.D. Thesis, Department of Mechanical Engineering, University of Waterloo, Waterloo, Canada.

Incropera, F. P., DeWitt, D. P., Bergman, T.L. and Lavine A. S., 2006, Fundamentals of Heat and Mass Transfer, Chapter 7, 6th edition, John Wiley & Sons. New Jersey: p. 402-411.

Kutscher, C.F., 1992, An investigation of heat transfer for air flow through low porosity perforated plates. Ph.D. Thesis, Department of Mechanical Engineering, University of Colorado at Boulder, Colorado, USA.

Kutscher, C.F., 1994, Heat exchanger effectiveness and pressure drop for air flow through perforated plates with and without crosswind, *J. Heat Transfer*, vol. 116: p. 391-399.

Kutscher, C.F., Christensen, C. and Barker, G., 1993, Unglazed transpired solar collectors: heat loss theory, *ASME J. Solar Eng*., vol. 115: p. 182-188.

Schlichting, H. and Gersten, K., 2000, Boundary layer theory, Chapter 15, 8th edition, Springer. New York: p. 457-460.

Van Decker, G.W. E., 1996, Asymptotic thermal effectiveness of unglazed transpired plate solar air heaters. M.A.Sc. Thesis, Department of Mechanical Engineering, University of Waterloo, Waterloo, Canada.

Van Decker, G.W. E., Hollands, K.G.T. and Brunger, A.P., 2001, Heat-exchange relations for unglazed transpired solar collectors with circular holes on a square or triangular pitch, *Solar Energy*, vol. 71: p. 33-45.